Advances in Water Resources 71 (2014) 125–139

Contents lists available at ScienceDirect

Advances in Water Resources

journal homepage: www.elsevier.com/locate/advwatres

An integral-balance nonlinear model to simulate changes in soil moisture, groundwater and surface runoff dynamics at the hillslope scale

Rodica Curtu [a,*], Ricardo Mantilla [b], Morgan Fonley [a], Luciana K. Cunha [b], Scott J. Small [b], Laurent O. Jay [a], Witold F. Krajewski [b]

[a] Department of Mathematics, The University of Iowa, Iowa City, IA 52242, USA
[b] IIHR – Hydroscience & Engineering, The University of Iowa, Iowa City, IA 52242, USA

ARTICLE INFO

Article history:
Received 27 June 2013
Received in revised form 9 May 2014
Accepted 2 June 2014
Available online 14 June 2014

Keywords:
Hillslope model
Surface vs. subsurface interactions
Nonlinear ODE system
Shale Hills watershed

ABSTRACT

We present a system of ordinary differential equations (ODEs) capable of reproducing simultaneously the aggregated behavior of changes in water storage in the hillslope surface, the unsaturated and the saturated soil layers and the channel that drains the hillslope. The system of equations can be viewed as a two-state integral-balance model for soil moisture and groundwater dynamics. Development of the model was motivated by the need for landscape representation through hillslopes and channels organized following stream drainage network topology. Such a representation, with the basic discretization unit of a hillslope, allows ODEs-based simulation of the water transport in a basin. This, in turn, admits the use of highly efficient numerical solvers that enable space–time scaling studies. The goal of this paper is to investigate whether a nonlinear ODE system can effectively replicate observations of water storage in the unsaturated and saturated layers of the soil. Our first finding is that a previously proposed ODE hillslope model, based on readily available data, is capable of reproducing streamflow fluctuations but fails to reproduce the interactions between the surface and subsurface components at the hillslope scale. However, the more complex ODE model that we present in this paper achieves this goal. In our model, fluxes in the soil are described using a Taylor expansion of the underlying storage flux relationship. We tested the model using data collected in the Shale Hills watershed, a 7.9-ha forested site in central Pennsylvania, during an artificial drainage experiment in August 1974 where soil moisture in the unsaturated zone, groundwater dynamics and surface runoff were monitored. The ODE model can be used as an alternative to spatially explicit hillslope models, based on systems of partial differential equations, which require more computational power to resolve fluxes at the hillslope scale. Therefore, it is appropriate to be coupled to runoff routing models to investigate the effect of runoff and its uncertainty propagation across scales. However, this improved performance comes at the expense of introducing two additional parameters that have no obvious physical interpretation. We discuss the implications of this for hydrologic studies across scales.

1. Introduction

Recent studies on the modeling of streamflow response to rainfall forcing using distributed hydrological models have revealed that model error decreases with increasing river basin scale [1,3,5,21]. This effect has been attributed to the averaging of errors in the distributed rainfall inputs and the attenuation effect of flows due to river routing [21,18]. However, the impact of that model structural error at the hillslope scale in determining errors as the river network aggregates flows is less understood. The contrasting results obtained in modeling catchments of different sizes motivate the investigation of the role of hillslope-model structure on error propagation across scales. An investigation of this nature requires the ability to address simultaneously the issue of fluxes draining out from millions of hillslopes (e.g., a 50,000 km^2 basin is constituted of approximately 1 million hillslopes according to [11]) and the difficulty of creating a hillslope scale model structure flexible enough to represent the complex dynamics that can occur at such scales. As a first step in this investigation, we develop and test in this paper a system of ordinary differential equations (ODEs) capable of replicating the integral behavior of water in the unsaturated and saturated soil layer in a hillslope as well as the behavior of the surface runoff. Our goal is to demonstrate that the dynamics described by

* Corresponding author. Tel.: +1 319 335 0744.
E-mail address: rodica-curtu@uiowa.edu (R. Curtu).

http://dx.doi.org/10.1016/j.advwatres.2014.06.003
0309-1708/

the ODE system are comparable to the dynamics described by a more complex partial differential equation (PDE) description of the system. This is important because several studies have demonstrated that spatially explicit models of hillslope processes, when properly parameterized, can capture simultaneously variations in the surface and dynamics of water in the soil [14,23]. However, the computational demands of simulating large areas ($\sim 10^5$ km^2) while preserving a sub-hillslope partitioning required by these models becomes a practical limitation. ODEs, on the other hand, can be solved very efficiently using parallel integrators [25].

Duffy [6] suggested (but has not tested) that using an integral-balance model for soil moisture and groundwater dynamics can yield comparable results. In this context, our goal is to address two open-ended questions raised by Duffy [6] related to the ability of simple low-dimensional models to capture the essential hydrologic processes involved based on a terrain averaging approach and integral-balance: (i) What should be considered an appropriate scale of aggregation? and (ii) Could low dimensional ODE models provide numerical results comparable to those obtained by more complex PDE-based models? If yes, to what kind of hydrologic data are these results relevant? Can they, for example, reproduce the dynamics of the water in the channel, the dynamics of groundwater, or both?

With regard to the first question, while we have not studied the issue in a systematic manner, we considered the hillslope scale proposed by Gupta and Wymire [12] to be an appropriate scale to describe the lumped behavior of the system. Specifically, we used data collected in The Shale Hills watershed, a 7.9-ha forested site in central Pennsylvania, during a comprehensive experiment on the role of soil moisture and runoff during the 1970s [17] (see description in Section 2) and show that ODE-based hillslope-scale models are able to reproduce certain aspects of water dynamics.

To address the second question, we use two ODE-based models that account for the interactions between atmospheric inputs and landscape properties, including soil, and their implications for the runoff transport dynamics (Section 3). Given that the Shale Hills watershed data set was used in previous studies [23] to examine the ability of the spatially explicit PIHM model, it constitutes an ideal test case to determine the extent to which ODE-based models can reproduce the behavior of water movements in a first order watershed. Numerical simulations and comparison with data, presented in Section 3.1, show that a simple model [4] with a parameterization based on commonly available data is skillful enough to reproduce streamflow fluctuations at the outlet of the basin, but it is not capable of correctly reproducing the dynamics of the surface and subsurface water interactions. By contrast, the more complex ODE-based nonlinear model developed here (see Sections 3.3 and 4) is indeed capable of achieving the same level of accuracy obtained by PDE-based models presented in the literature [15,23]. The price for the improved performance is the introduction of two parameters that have no obvious physical interpretations.

Results of our ODE model are just an intermediate, but nevertheless essential, piece of information that will be later integrated into a larger project. To this end, our longer-term goal is to determine whether or not a complex hillslope model is a necessary condition for accurate simulations of streamflow fluctuations in larger basins (>100 km^2). Our most recent experiences in simulating streamflow fluctuations across multiple scales suggest that the answer is "no." We return to these questions in Section 5 with conclusions of the work and a discussion of future directions.

2. Description of data and site information

The Shale Hills watershed is a 7.9-ha (19.8-acre) forested site in central Pennsylvania. It was the subject of a comprehensive experiment on the role of soil moisture and runoff during the 1970s [17]. Steep slopes and narrow ridges typical of the valley and ridge province characterize this first-order drainage basin. The permeable forest soils are uniform in thickness with an average depth of 1.4 m [16]. Underlying the soil is a thick shale bedrock with interbedded limestone, which is thought to have low permeability [16].

A relatively detailed description of the Shale Hills field experiment that was conducted during the year 1974 can be found in [23]. We focus here exclusively on the data from a shorter time interval, 31 days in the month of August. The data were collected at the outlet weir (flow values in m^3/s) and other three weirs, and at 40 piezometers, 40 neutron access probes for soil moisture distributed along the hillslope. Then, storage of soil moisture and saturated groundwater changes were estimated during a series of artificial rainfall experiments (see Table 1 based on data from [13]). A spray irrigation network was implemented to allow for a control on the irrigation events. During the month of August 1974, six equal artificial rainfall events of about $p(t) = 6.4$ mm/h for 6 h were applied below the tree canopy, while some other natural rain events occured during the month. (This natural precipitation will also be included in the ODE modeling process.) The six controlled rain events were applied to the entire watershed [23] during the following days and starting with the following hours: 8/1/1974 at 6:45 AM ($t = 405$ min), 8/7/1974 at 7:15 AM ($t = 9075$ min), 8/14/1974 at 7:15 AM ($t = 19155$ min), 8/19/1974 at 7:15 AM ($t = 26355$ min), 8/23/1974 at 8:30 AM ($t = 32190$ min), and 8/27/1974 at 7:45 AM ($t = 37905$ min). See [13] and Appendix A for more details on data. Note that our selection of units in the vertical and horizontal (time) axes in the figures was made to facilitate the comparison with results by Qu and Duffy [23].

3. Modeling of the hillslope-river channel coupling

The model is a system of four ODEs that account for the interactions between atmospheric inputs and landscape properties and their implication with respect to the runoff transport dynamics. We acknowledge that, by working with an ODE framework, the hillslope-channel coupling physical processes are simplified in description (as all variables account only for spatially averaged variables and processes). Nevertheless, this formulation is advantageous because it allows for a systematic investigation of how different fluxes involved in the runoff production and runoff transport contribute to the ultimate dynamics of the water in the channel. We take advantage of existing soil and runoff data in a one-month experiment in the Shale Hills watershed in order to test this ODE-based approach and to show that it captures the most relevant aspects of the dynamical evolution of the system.

Four physical control volumes are considered: (1) the water that is ponded, but still mobile, in the hillslope surface, which will either infiltrate into the soil matrix or drain as surface runoff, (2) the unsaturated portion of the soil matrix; (3) the corresponding saturated portion and, lastly; (4) the water stored in the channel link that drains the entire hillslope area (see Fig. 1). The soil matrix is assumed to have a finite capacity, and the unsaturated and saturated zone control volumes are therefore dynamic in size. Fluxes among these four control volumes are limited to $Q_{p,l}$ and $Q_{p,u}$ from ponded to the channel link and to the unsaturated zone, respectively, $Q_{u,s}$ the flux exchange between the unsaturated and saturated zones and $Q_{s,l}$ subsurface runoff into the channel link.

3.1. An initial attempt: a calibration-free integral-balance ODE system fails to reproduce the soil moisture data, at hillslope-scale

In our quest for the construction of an ODE model at the hillslope-scale that is completely free of calibration, we have initially considered the model introduced in [4]. This system of

Table 1
(Columns C1–C5): Soil data from the Shale Hills experiment during the month of August 1974 [13]; (Columns C6–C8): Time (in minutes) and the averaged values of both north and south slopes data, calculated in meters – 0.0254(C2 + C3)/2 and 0.0254(C4 + C5)/2 respectively.

Time (h)	Saturated storage (in)		Unsaturated moisture (in)		Time (min) $\times 10^4$	Hillslope average	
	North	South	North	South		Saturated storage (m)	Unsaturated moisture (m)
12.25	9.13	6.21	11.36	9.01	0.074	0.19	0.26
33.50	9.50	3.81	11.53	9.81	0.201	0.17	0.27
57.50	9.53	1.23	11.38	10.54	0.345	0.14	0.28
105.50	8.40	1.36	11.96	10.85	0.633	0.12	0.29
129.50	8.01	0.70	11.94	11.02	0.777	**0.11**	0.29
156.75	9.66	11.24	11.45	7.11	0.941	0.27	0.24
182.50	9.81	6.82	11.41	9.10	1.095	0.21	0.26
207.00	9.05	4.40	11.64	9.94	1.242	0.17	0.27
277.50	7.83	2.09	12.21	11.05	1.665	0.13	**0.30**
301.50	7.81	1.75	11.94	11.11	1.809	0.12	0.29
326.00	12.22	14.19	10.87	6.36	1.956	0.34	0.22
350.00	12.07	6.83	10.94	9.24	2.100	0.24	0.26
374.00	10.74	4.18	11.46	9.85	2.244	0.19	0.27
422.00	9.13	2.29	11.75	10.74	2.532	0.15	0.29
446.50	10.96	14.32	11.31	5.62	2.679	0.32	0.21
472.50	11.72	7.24	11.20	8.88	2.835	0.24	0.25
496.50	10.48	3.78	11.53	10.26	2.979	0.18	0.28
520.50	9.76	2.83	11.87	10.80	3.123	0.16	0.29
544.00	13.92	15.61	9.42	4.27	3.264	0.38	0.17
569.00	13.03	8.28	10.35	8.14	3.414	0.27	0.23
615.00	9.98	4.00	11.71	10.18	3.690	0.18	0.28
638.00	13.61	15.48	10.03	4.49	3.828	0.37	0.18
687.50	12.21	6.87	10.82	8.46	4.125	0.24	0.24

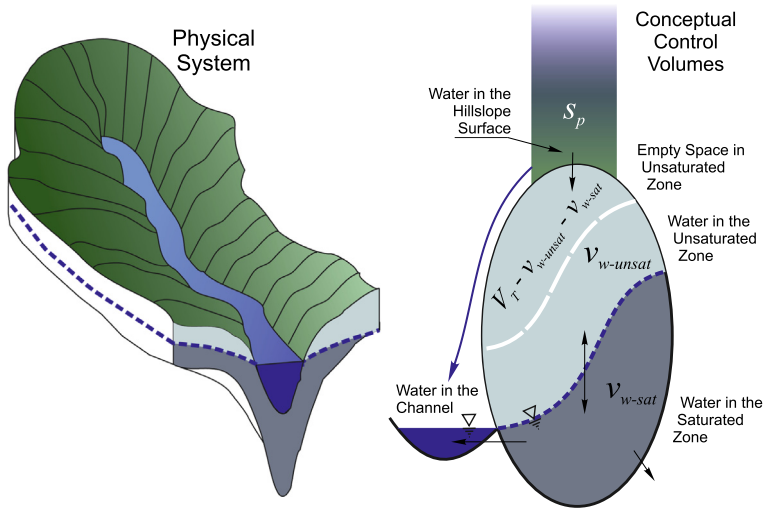

Fig. 1. Conceptual model.

ordinary differential equations is also based on the physical properties of the hillslope-channel coupling and has all its parameters determined from digital elevation models (DEM), geological maps and some theoretical considerations. Moreover, when simulated for large-scale river networks, it shows good approximation of flow data [4].

Given that the model from [4] is not the focus of our paper, and to ensure completion, we only summarize its equations below and list its fluxes and parameter values in Appendix B

$$\begin{aligned}
\frac{ds_p}{dt} &= c_7(p - e_p - q_{pl} - q_{pu}),\\
\frac{dv}{dt} &= c_8(q_{pu} - q_{us} - e_{unsat}),\\
\frac{da}{dt} &= c_8(q_{us} - q_{sl} - e_{sat}),\\
\frac{d(qQ_r)}{dt} &= K_Q\, q^{\lambda_1}\left(-qQ_r + q_{in}Q_r + c_4(q_{pl} + q_{sl})\right).
\end{aligned} \tag{1}$$

The variables are: s_p the surface ponding water in (mm); $v = v_{w\text{-}unsat}/A_H$ the average storage of soil moisture in (m); $a = v_{w-sat}/A_H$ the average saturated soil storage in (m); and qQ_r is the channel discharge measured in (m^3/s). Here $Q_r = 1\ m^3/s$ is a normalization constant; A_H is the hillslope area; t represents the time measured in minutes; and K_Q is the river network transport constant.

Note that the volume of water in the unsaturated layer of soil depends on the dimensionless soil volumetric water content θ through the formulation $v_{w\text{-}unsat} = \theta v_{s\text{-}unsat} = \theta h_b a_P$, where a_P is the permeable area and h_b is the effective soil depth. Likewise, variable a depends on the water table h_w according to the formula $a = v_{w-sat}/A_H = v_{s-sat}/A_H = h_b \mathcal{P}(\frac{h_w - h_b}{H_h})$. where $\mathcal{P}$ is a third degree polynomial with coefficients derived from DEM (see Appendix B) and H_h is the hillslope relief. The fluxes from the equations (all are expressed in "per unit area" units) stand for: q_{pl} is the flux from the surface to the channel, in (mm/h); q_{pu} is the flux from surface to

soil, in (mm/h); q_{us} is the flux from the unsaturated layer to the saturated zone, in (mm/h); and q_{sl} is the flux from the saturated layer to the channel, in (mm/h); $p(t)$ is precipitation in (mm/h); and $e_p(t)$, $e_{sat}(t)$, $e_{unsat}(t)$ are the evaporation rates from the surface, the saturated layer and the unsaturated layer, in (mm/h). An important observation is that the system (1) fails to reproduce at a reasonable level the soil moisture data when applied to the local, hillslope-scale; see Fig. 2 for a comparison of the numerical simulation and data in the Shale Hills watershed.

Fig. 2 shows that the model is able to reproduce channel discharge at the outlet with reasonable accuracy but fails to represent soil dynamics between the saturated and unsaturated layers. This limitation arises mainly from the fact that the model does not account for soil dynamic thresholds that are evident in the observed data. The first threshold can be identified on the unsaturated portion of the soil. There seems to be a maximum value of unsaturated water volume (0.3 m) that activates the flow from the unsaturated to the saturated layer – see also Table 1. Another threshold is in the saturated portion of the soil that presents a minimum water table close to 0.1 meters. These thresholds are not well understood and are difficult to estimate in the absence of soil data.

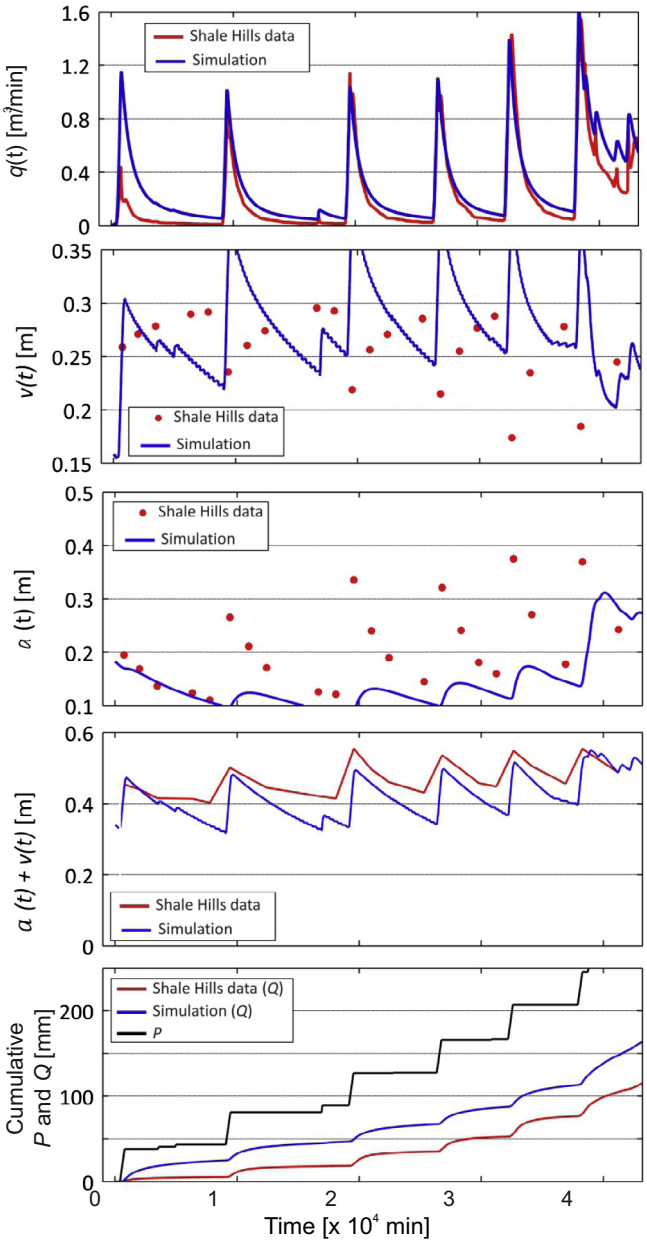

Fig. 2. Numerical simulations of system (1) and comparison with the Shale Hills watershed data for flow qQ_r measured in (m^3/min), and water level in the unsaturated and saturated zones, in (m).

Consequently, we are still in need of a nonlinear (calibration-free to the maximum extent) ODE model that corrects the observed errors and that can still be easily included in simulations of increasing river basin scale. This goal is achieved through system (2) and (3) described below.

3.2. A new formulation: an integral-balance ODE system that captures the soil moisture data at hillslope-scale

This nonlinear ODE model assumes four variables s_p, v, a and q (summarized in Table 2) that change with respect to time, which is measured in minutes. In terms of fluxes, the system is defined as

$$\begin{aligned}
&\frac{d(s_p A_H)}{dt} = (1-E(t))A_H\,p(t) - Q_{p,l} - Q_{p,u},\\
&\frac{d(v_{w\text{-}unsat})}{dt} = \frac{d(\beta v A_H)}{dt} = Q_{p,u} - Q_{u,s},\\
&\frac{d(v_{w\text{-}sat})}{dt} = \frac{d(\beta a A_H)}{dt} = Q_{u,s} - Q_{s,l} - Q_{evap},\\
&\tau\frac{d(qQ_r)}{dt} = q^{\lambda_1}\left(-qQ_r + q_{in}Q_r + Q_{p,l} + Q_{s,l}\right),
\end{aligned} \tag{2}$$

where A_H is the total hillslope area, $p(t)$ is the precipitation input in (mm/h) and $E(t)$ represents the percentage of total (incoming) water loss due to rapid evaporation from the surface or interception by vegetation. The flux Q_{evap} accounts for the potential loss of groundwater through evaporation or plant consumption or both.

The runoff transport in the channel that drains the hillslope is modeled by the non-linear reservoir equation that was derived by Mantilla [19] and based on previous works by Gupta and Waymire [12], Reggiani et al. [24] and Menabde and Sivapalan [22]. Here the changes in water mass in a channel link are determined by incoming fluxes from upstream channel-links (q_{in}), the lateral runoff from the hillslope (overland flow $Q_{p,l}$ and groundwater flow from the saturated zone $Q_{s,l}$) and the outgoing discharge Q. Therefore, the variable q is defined as $q = Q/Q_r$ where $Q_r = 1\ m^3/s$ is the unit reference discharge. The incoming flux q_{in} is either zero (for first-order drainage basins, as is the case for the Shale Hills watershed) or it represents the sum of surface fluxes from the incoming channel-links $q_{in} = \sum_{j\in Upstream(q)} Q_j(t)/Q_r$.

Note that in order to account for heterogeneities in the soil matrix that make certain portions inaccessible to water, such as the space occupied by tree roots, an adjustment coefficient β is introduced. Thus, the volume of water in the unsaturated and saturated zones are defined by $v_{w\text{-}unsat} = \beta(\theta v_{unsat})$ and $v_{w-sat} = \beta v_{sat}$ where $\theta \in [0,1]$ represents the volumetric water content (soil moisture). The variables a and v are strongly linked because of the finite storage capacity of the hillslope. We assume an effective soil depth h_b over the total hillslope area A_H such that the total volume of the hillslope is $V_{tot} = h_b A_H$. Given the high density of tree roots in the Shale Hills watershed, we note that the total volume of the hillslope effectively available for water is only a percentage of V_{tot}, say $V_T = \beta V_{tot} = \beta h_b A_H$ with $\beta \in (0,1]$. The saturated zone a_l is a percentage of the total hillslope area, and it can be defined as $a_l = \hat{a}A_H$ with $0 \leqslant \hat{a} \leqslant 1$. Then, the volume of the saturated zone is $v_{sat} = a_l h_b$. With notation $a = \hat{a}h_b$, we obtain that the volume of water in the saturated zone is $v_{w-sat} = \beta v_{sat} = \beta a A_H$ and a can take only values between zero and h_b. Similarly, with notation $v = \theta(1-\hat{a})h_b$, the volume of water in the unsaturated zone is $v_{w\text{-}unsat} = \beta(\theta v_{unsat}) = \beta\theta(V_{tot} - v_{sat}) = \beta v A_H$ and $0 \leqslant v \leqslant h_b - a$.

Table 2
Variables of the nonlinear ODE model.

Variable	Unit	Definition	Physical interpretation
s_p	m	$s_p = v_{w\text{-}ponded}/A_H$	The volume per unit hillslope area of water stored in the ground surface, or ponded water
v	m	$v = \theta v_{unsat}/A_H$	The volume per unit hillslope area of moisture content in the unsaturated zone
a	m	$a = v_{sat}/A_H$	The volume per unit hillslope area of the saturated zone
q	None	$q = Q/Q_r$	The flow going downstream out of the channel at time t. Q is the runoff at the outlet (in m^3/s) and Q_r is the unit reference discharge, $Q_r = 1\ m^3/s$

3.3. Definition of the nonlinear ODE model

The nonlinear model for the local runoff-production and runoff-transport consists of four ODEs that result from (2) with fluxes defined by Table 3. This is

$$\begin{aligned}
\frac{ds_p}{dt} &= [1-E(t)]c_3\,p(t) \\
&\quad - c_1 s_p(a-a_{res}+v-v_{res}) - c_1 s_p[h_b-(a-a_{res})-(v-v_{res})] \\
\beta\frac{dv}{dt} &= c_1 s_p\,[h_b-(a-a_{res})-(v-v_{res})] \\
&\quad - \left[d_0(v-v_{res}) + d_1(v-v_{res})(a-a_{res})^2 + d_2(a-a_{res})^2\right] \\
\beta\frac{da}{dt} &= \left[d_0(v-v_{res}) + d_1(v-v_{res})(a-a_{res})^2 + d_2(a-a_{res})^2\right] \\
&\quad - c_2\,(a-a_{res})\,\exp\left(\alpha_N\frac{a-a_{res}}{h_b}\right) - c_{evap}\,(a-a_{res}) \\
\tau\frac{dq}{dt} &= q^{\lambda_1}\left[q_{in}-q+\gamma c_1 s_p\,(a-a_{res}+v-v_{res})\right. \\
&\quad \left.+\gamma c_2\,(a-a_{res})\,\exp\left(\alpha_N\frac{a-a_{res}}{h_b}\right)\right]
\end{aligned} \tag{3}$$

with parameters $\beta, h_b, a_{res}, v_{res}, d_0, d_1, d_2, \lambda_1, \alpha_N$ and function $E(t)$ as in Table 4 and $c_1, c_2, c_3, c_{evap}, \gamma, \tau$ defined indirectly according to the formulas

$$\begin{aligned}
&c_1 = \frac{K_{s_p}}{60\,h_b}\quad (m^{-1}\ min^{-1}),\quad c_2 = \frac{10^{-6}\,\alpha_{soil}K_{SAT}\,(2L)}{60\,A_H}\quad (min^{-1}),\\
&c_3 = \frac{10^{-3}}{60}\quad (\text{no unit}),\quad c_{evap} = \frac{K_{evap}}{60}\quad (min^{-1}),\\
&\gamma = \frac{10^6 A_H}{60\,Q_r}\quad (m^{-1}\ min),\quad \tau = \frac{(1-\lambda_1)L}{60\,v_r\,(A_{upstream}/A_r)^{\lambda_2}}\quad (min).
\end{aligned} \tag{4}$$

The hillslope reference area $A_r = 1\ km^2$ is a normalization constant that we introduced with the goal of adjusting certain physical units. The parameter τ is the scale-dependent residence time for the channel discharge (in minutes), and it equals the inverse of the river network transport constant, $\tau = K_Q^{-1}$ [19]. Scale dependency is established here by the upstream area, which reflects changes in the hydraulic geometry in the downstream direction. We will demonstrate later in the paper that, at the scales considered here, the effect of the attenuation in the channel is negligible compared to the effects of hillslope dynamics.

A justification of the particular mathematical description of fluxes $Q_{p,l}$, $Q_{p,u}$, $Q_{s,l}$ and Q_{evap} is included in C. However, we explain here the mathematical basis for our choice of $Q_{u,s}$, the flux between the unsaturated and saturated zones.

Since the interaction between the two volumes of water v_{unsat} and v_{sat} is not static (on the contrary, it is obtained through a moving interface), we anticipate that higher nonlinearities may play an important role. Assuming everywhere a local interaction between the two layers of water in the soil, we take the entire hillslope area A_H as sectional area. This, together with a nonlinear velocity $vel = vel(v,a)$, defines the flux $Q_{u,s}$ as a product, $Q_{u,s} = A_H\,vel(v,a)$.

Let us assume $vel(v,a)$ is a general nonlinear function in variables a and v such that $vel = 0$ at the equilibrium point (a_{res}, v_{res}). Then its Taylor expansion about the equilibrium is $vel(a,v) = \eta_{10}(a-a_{res}) + \eta_{01}(v-v_{res}) + \eta_{20}(a-a_{res})^2 + 2\eta_{11}(a-a_{res})(v-v_{res}) + \eta_{02}(v-v_{res})^2 + \eta_{30}(a-a_{res})^3 + 3\eta_{21}(a-a_{res})^2(v-v_{res}) + 3\eta_{12}(a-a_{res})(v-v_{res})^2 + \eta_{03}(v-v_{res})^3 + \cdots$ with coefficients $\eta_{ij} = \frac{1}{(i+j)!}\frac{\partial^{i+j}vel}{\partial^i a\,\partial^j v}$ computed at (a_{res}, v_{res}). Then, the form of the function $vel = vel(a,v)$ that we use for our model can be interpreted as a particular choice taken from the class of nonlinear functions that describe well the flux between the unsaturated and saturated zones and that could be empirically determined when studying certain hillslopes.

Here, we adopt a formulation of the velocity similar to Duffy's work from [6], and take $vel(a,v) = d_0(v-v_{res}) + d_1(v-v_{res})(a-a_{res})^2 + d_2(a-a_{res})^2$ obtaining $Q_{u,s}$ as in Table 3. Note that d_0, d_1, d_2 are positive parameters that depend (in a complex way, not identified in this paper) on properties of the hillslope and soil. such as the shape of the hillslope (e.g. its convexity), the soil conductivity and its capillarity.

3.4. Measurable and non-measurable model parameters

An important component of our approach is the goal to reduce, as much as possible, the number of non-measurable model parameters. The parameters are grouped into three main categories (see Table 4): (i) derivable directly from DEM and geological maps; (ii) derivable from independent empirical observations and (iii) estimated from local observations of state variables. A detailed

Table 3
Definition of fluxes in the nonlinear ODE model.

Formula	Physical interpretation
$Q_{p,l} = c_1 A_H s_p(a-a_{res}+v-v_{res})$	Flux from ponded water to the channel link (surface runoff)
$Q_{p,u} = c_1 A_H s_p[h_b-(a-a_{res})-(v-v_{res})]$	Flux from ponded water to the unsaturated zone (infiltration)
$Q_{u,s} = A_H[d_0(v-v_{res}) + d_1(v-v_{res})(a-a_{res})^2 + d_2(a-a_{res})^2]$	Flux exchange between the unsaturated and saturated zones (recharge)
$Q_{s,l} = c_2 A_H\,(a-a_{res})\,\exp\left(\alpha_N\frac{a-a_{res}}{h_b}\right)$	Flux for subsurface runoff into the channel link (baseflow)
$Q_{evap} = c_{evap} A_H\,(a-a_{res})$	Flux for the potential loss of groundwater through either evaporation or plant consumption

Table 4
Parameters in the nonlinear ODE model that are: (i) derivable directly from DEM and geological maps; (ii) derivable from independent empirical observations; and (iii) estimated from local observations of state variables.

Parameter	Physical interpretation
Parameters derivable directly from DEM and geological maps	
$A_{upstream}$	Total upstream area determined from DEM with typical values in the interval $[0.01\ \text{km}^2, 10^6\ \text{km}^2]$. Note: $A_{upstream} = A_H$ for order 1 links
A_H	Total hillslope area determined from DEM with typical values in the interval $(0\ \text{km}^2, 5\ \text{km}^2]$
L	The channel (link) length determined from DEM with typical values in the interval [10 m,1000 m]
h_b	The effective soil depth to the impermeable layer with typical values in the interval (0 m,0.8 m]. Note: h_b incorporates information about the soil porosity (e.g. for averaged physical soil depth to the bedrock $h_{sd} = 1.4$ m and porosity $\pi = 0.4$, we have $h_b = h_{sd} \times \pi = 0.56$ m)
Parameters derivable from independent empirical observations	
λ_1	The nonlinear exponent for flow velocity function-discharge with typical values in the interval $[0.05, 0.7]$
λ_2	The nonlinear exponent for flow velocity function-upstream area with typical values in the interval $[-0.4, -0.05]$
v_r	The reference flow velocity, a constant determined from the channel geometry and flow measurement data with typical values in the interval [0.2 m/s,1 m/s]
K_{SAT}	The saturated hydraulic conductivity with typical values in the interval $[10^{-6}\ \text{m/h}, 1\ \text{m/h}]$
$d_0,\ d_1,\ d_2$	Parameters that describe the form of the hillslope-scale recharge relation coupling the state variables
Parameters that are estimated from local observations of state variables	
$a_{res},\ v_{res}$	The residual storage volumes for the gravity-drained hillslope
β	Parameter that accounts for the heterogeneities in the soil matrix porosity and areas inaccessible to water (e.g. portions of soil matrix occupied by tree roots, gravel, etc); $\beta \in (0, 1]$
α_N	Parameter that controls the recession
α_{soil}	Heterogeneity factor for soil saturated hydraulic conductivity
K_{s_p}	Parameter that characterizes the overland flow to the channel and the infiltration to the soil
K_{evap}, E	Parameters that correspond to the evaporation process and water consumption by vegetation

explanation of how their values are chosen is given in Section 4.1. Essentially, in model (3), the majority of the parameter values are not subject to calibration. Only a subset of parameters (α_{soil} and K_{s_p}) still remains unconstrained and has been used in the fitting of the numerical simulation. The latter are considered to represent general characteristics of the hillslope. The values of the unconstrained parameters are estimated for one event and are to be left unchanged in any other simulations of the model subject to new precipitation input patterns. On the other hand, two other parameters of the ODE model which are related to evapotranspiration (K_{evap} and E) are adjusted for every rain event, but their values are chosen in accordance with the data to match the observed water balance (see Section 4.1).

4. Numerical simulations and interpretation of the results

We test the nonlinear ODE system using data from the Shale Hills experiment that was conducted in August 1974 (data obtained by courtesy of Duffy and collaborators [13]). These data were previously used to generate and test a multi-process watershed simulation based on PDE formulation [23] whose numerical integration, however, poses several difficulties and requires significant time.

Our goal is to show that the simple ODE system given by (3) can reproduce data as closely as the PDE model when spatial averaging is considered along the hillslope. The state variables considered here are streamflow at the outlet weir (flux q), the total volume of water in the soil, both in the unsaturated zone (v) and the saturated zone (a). We are particularly interested in simulating the observed double peak in the hydrograph created after each rainfall event (See Figs. 3 and 4). The appearance of the double peak in the ODE model is especially interesting as, at the very least, it provides an alternative to the hypothesis that the double peak should be the result of the hillslope's complex topography. The latter would have led to different time-delays for the overland or underground flows on the north and south slopes, respectively, and that could have presumably been reproduced only by a detailed spatial description of the hillslope that only a PDE model could achieve. On the contrary, the appearance of the double peak in the spatially averaged ODE model points to the interaction between the hillslope overland runoff and the subsurface flow. Those seem to be subject to a delicate balance in order to produce the double peak.

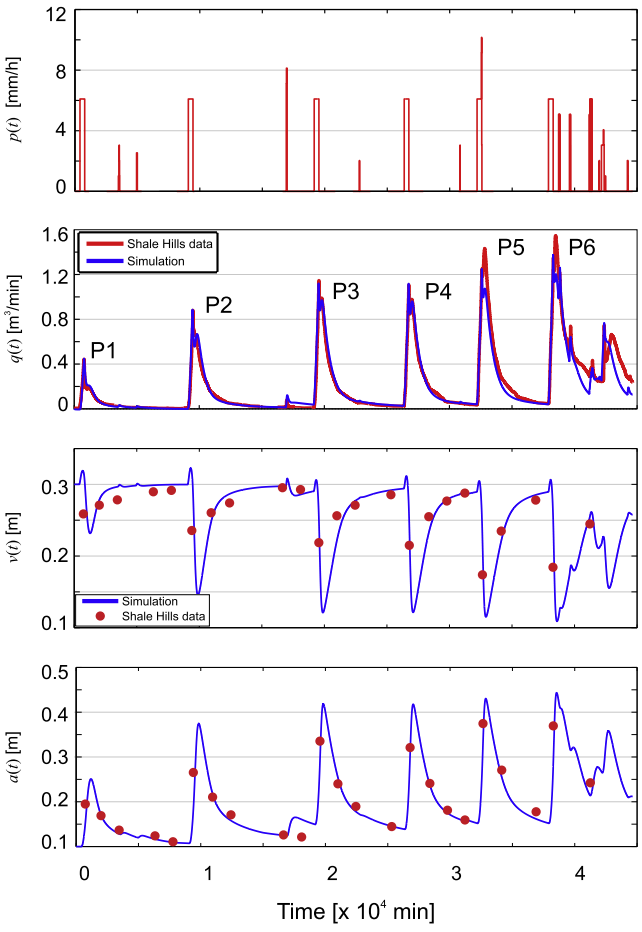

Fig. 3. Simulations of the nonlinear ODE model (3) with parameters and initial conditions from Section 4.1, and comparison to data from the Shale Hills experiment for the month of August 1974 ([13]; see also columns 6–8 in Table 1).

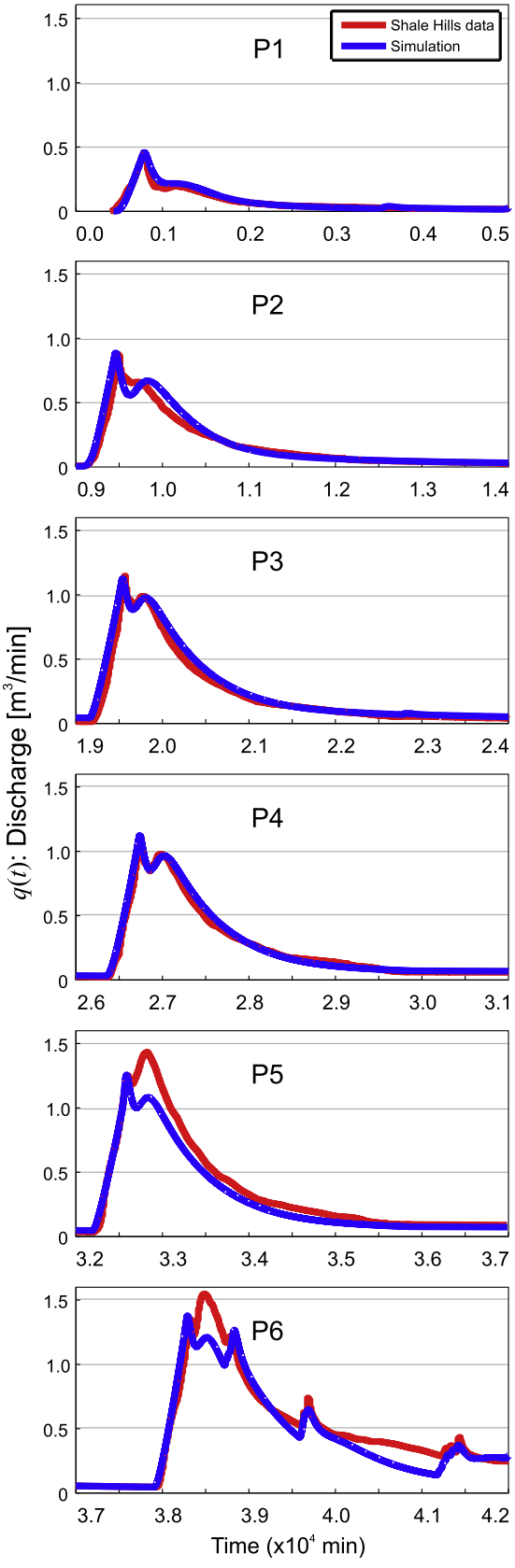

Fig. 4. Zoom in at peaks 1–6 of the output flow $Q = qQ_r$ measured in m^3/min, during the six forced rain events of the Shale Hills experiment of August 1974. Comparison of data (solid red) and simulated output flow of model (3) with parameter values and initial conditions from Section 4.1 (solid blue). See also Fig. 3 (second panel). (For interpretation of the references to color in this figure caption, the reader is referred to the web version of this article.)

The ODE model can also capture the qualitative and the quantitative dynamics of the underground water and offer a possible interpretation of how water is redistributed between the saturated and unsaturated zones in the period between successive rainfall events (see Fig. 3 (panels 3–4) and Table 1).

4.1. Parameter values and initial conditions

Our aim is to present an ODE model that is not only relevant at the hillslope scale but that also steers clear of calibration to the greatest possible extent. With this idea in mind, we determine the values of parameters $A_{upstream}$, A_H, L and h_b directly from DEM and geological maps for the Shale Hills watershed [13]; see Table 5. For example, h_b results from calculated averaged soil depth $h_{sd} = 1.4$ m of the hillslope and porosity factor $\pi = 0.4$ [19,20].

Other parameters are evaluated based on theoretical considerations; we chose the values of parameters $\lambda_1, \lambda_2, v_r$ as indicated by [19,20], and the values of K_{SAT} and d_0, d_1, d_2 as suggested by [2,6]. Note, for example, that the ODE model (3) does not show any significant sensitivity to the values chosen for λ_1, λ_2 and v_r in their corresponding range found in [19,20]. The rest of the parameters are estimated from local observations of state variables, as follows. The residual values for water in the soil a_{res} and v_{res} were chosen through a visual inspection of the soil data (see Table 1 and lower panels from Fig. 3) and indicate a tendency of the saturated and unsaturated water levels to relax to approximately the same numbers after the forced rain event passed and was followed by several days of no precipitation. We chose a_{res} close to the minimum value for the saturated storage area (column 7) and v_{res} close to the maximum value for the unsaturated area moisture (column 8) from Table 1 and hypothesized them to be steady-states for our variables a and v in the ODE model. We say that a_{res} and v_{res} are the residual storage volumes for gravity-drained hillslope (determined asymptotically, at zero precipitation). The value for β is chosen based on data analysis in order to ensure a closed water-balance of the hydrological system (see Appendix A for more details). The value for α_N is determined such that the model follows the trend of recession in flow data. Then, only two parameters K_{s_p}, and α_{soil} remained open for calibration and were used in the fitting of soil and flow data from [13] – see Table 5 for their determined values.

Table 5
Parameter values used in the numerical simulations of the nonlinear ODE model.

Parameter	Value	Unit
Parameters derivable directly from DEM and geological maps		
$A_{upstream}$	0.07736	km^2
A_H	0.07736	km^2
L	420.15	m
h_b	0.56	m
Parameters derivable from independent empirical observations		
λ_1	0.25	
λ_2	−0.1	
v_r	0.66	m/s
K_{SAT}	0.01	m/h
d_0	0.00135	min^{-1}
d_1	0.016	$m^{-2}\ min^{-1}$
d_2	0.0053	$m^{-1}\ min^{-1}$
Parameters that are estimated from local observations of state variables		
a_{res}	0.1	m
v_{res}	0.3	m
β	0.12	
α_N	2.5	
Parameters that cannot be estimated a priori		
α_{soil}	5.0	
K_{s_p}	0.625	h^{-1}

In addition, the evaporation from the surface (as a fraction) is taken to vary during the month of August, with higher values at the beginning and lower values later in the month: $E(t) = 0.62$ if $0 \leqslant t < 5000, 0.48$ if $5000 \leqslant t < 18,000, 0.50$ if $18,000 \leqslant t < 25,000, 0.48$ if $25,000 \leqslant t < 30000, 0.51$ if $30,000 \leqslant t < 35,000$, 0.44 if $35000 \leqslant t < 40,000$ and 0.3 if $t \geqslant 40,000$ ([13,10]; see also A for data analysis that suggests an average $1 - E(t) = \alpha(t) \approx 0.52$ during the precipitation events). On the other hand, the evaporation from the soil (water uptake by plant roots) in the saturated zone is also taken to vary during the month, with decreasing values toward the end of it: $K_{evap}(t) = 0.002$ if $0 \leqslant t < 8000$, then 0.0005 if $8000 \leqslant t < 15,000$, then 0.0001 if $15000 \leqslant t < 30,000$ and 0.0 for $t \geqslant 30,000$.

Our simulations were conducted in XPPAUT [7] using a Runge–Kutta numerical method with stepsize $\Delta t = 0.05$ mins and then checked for stability of the solution. The initial conditions were chosen at steady state for soil ($s_p(0) = 0$ m, $a(0) = 0.1$ m, $v(0) = 0.3$ m) and based on the Shale Hills data for the flow at the outlet weir at 12:00 AM on August 1st, 1974 ($q(0) = Q(0)/Q_r$, dimensionless, corresponding to $Q(0) = 9.31 \times 10^{-5}$ m^3/s). The results of the simulations and a comparison to data are shown in Fig. 3, where we plot variables v, a (in meters) and $Q = qQ_r$ (in units adjusted to m^3/min).

4.2. Interpretation of the numerical results

4.2.1. Water dynamics in the soil

Our initial observation is that the data for the saturated and unsaturated soil is well captured by the ODE model (Fig. 3, panels 3–4). The unsaturated zone experiences an increase in water volume during each rain event; however, this is followed by a sudden loss of water due to a fast flow into the saturated zone. This fast flow pushes the water level v below its equilibrium value v_{res}, while water in the saturated zone (variable a) rapidly increases above a_{res}. Between two consecutive rain events, the flux $Q_{u,s}$ decreases and then changes signs (it becomes negative), which allows for the redistribution of water in the soil before reducing to zero (see Fig. 5f for a graph of $vel = Q_{u,s}/A_H$). Both unsaturated and saturated water levels v, a relax back to their equilibrium values v_{res}, a_{res}, with an increasing trend for v and a decreasing trend for a (Fig. 3).

Mathematically, these dynamics can be explained through the presence of the nonlinear terms in the definition of $Q_{u,s}$ (see Table 3). If, for instance, at the beginning of the rain event the soil was at equilibrium ($v = v_{res}$ and $a = a_{res}$) so $Q_{u,s} = 0$. As $Q_{p,u}$ increases due to rain, v increases as well ($v > v_{res}$) but is still in the neighborhood of v_{res}; the higher order terms in $Q_{u,s}$ are negligible by comparison to the linear term $d_0(v - v_{res})$, so $Q_{u,s}$ starts to increase ($Q_{u,s} > 0$). As a consequence, a increases as well, which contributes to the changes of $Q_{u,s}$; the greater the increase in a, the faster the transfer of water from the unsaturated zone to the saturated zone (according to the quadratic term $d_2(a - a_{res})^2$). Thus, $Q_{u,s}$ eventually balances and overcomes the incoming flux $Q_{p,u}$ from the ponded water; this leads to a decrease in v that accelerates when rain stops (when $Q_{p,u} = 0$) pushing v below its equilibrium level ($v < v_{res}$). The cubic term $d_1(v - v_{res})(a - a_{res})^2$ which is dominant now in the definition of $Q_{u,s}$ takes negative values; consequently, $Q_{u,s}$ slows down and eventually reverses direction, moving water from the saturated zone back to the unsaturated zone ($Q_{u,s} < 0$). Thus, v increases back to v_{res} while a decreases towards a_{res}.

Note that the ODE model effectively captures the qualitative and quantitative dynamics of the water levels in the soil (both unsaturated and saturated). The nonlinear definition of both $Q_{u,s}$ and $Q_{s,l}$ fluxes contribute significantly to this result. The decaying slope for a, but also the increasing slope for v, are especially well adjusted due to the high nonlinearity of function $\mathcal{F}(x) = xe^{\alpha_N x}$ (see Fig. 5e for $Q_{s,l}/A_H$).

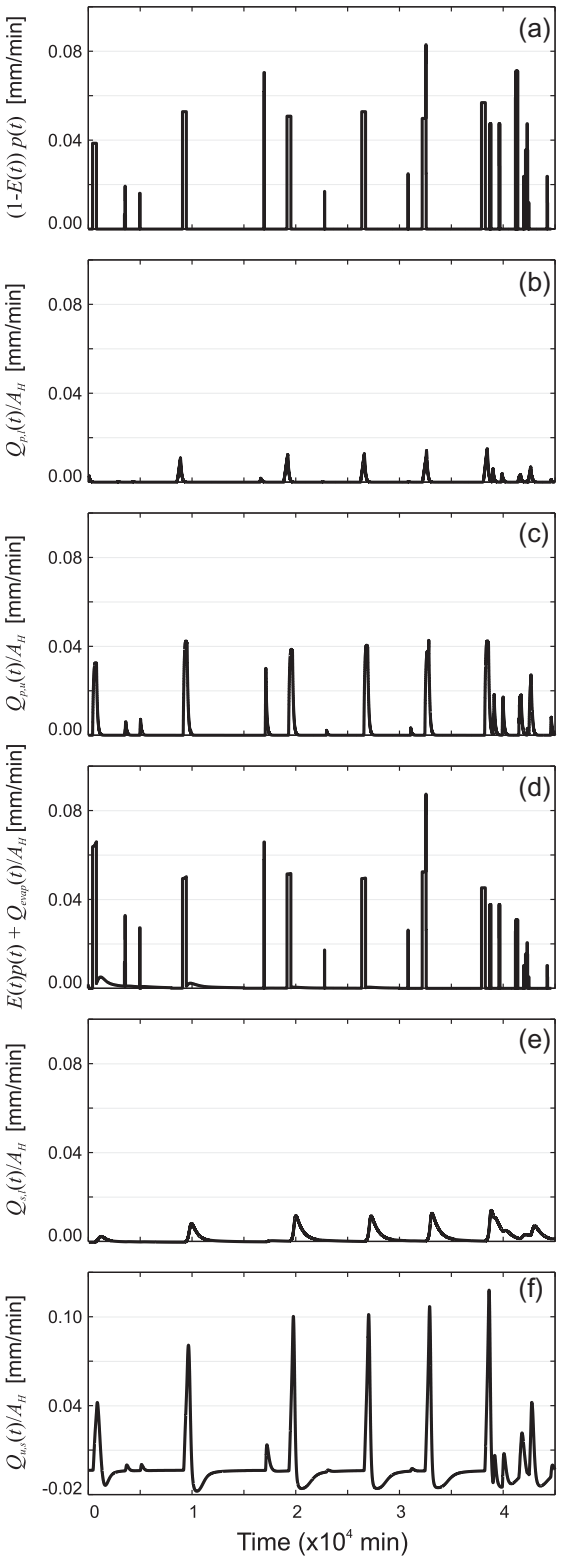

Fig. 5. Overland and underground fluxes (per hillslope area unit, Q_{ij}/A_H; measured in mm/min) determined by simulation of the model (3).

4.2.2. Overland flow dynamics

The dynamics of the main fluxes involved in the s_p-equation are shown in Fig. 5. As expected, the ponded water s_p increases during each precipitation event and rapidly goes to zero when rain stops; since fluxes $Q_{p,l}$ and $Q_{p,u}$ depend linearly on s_p, they also reach zero

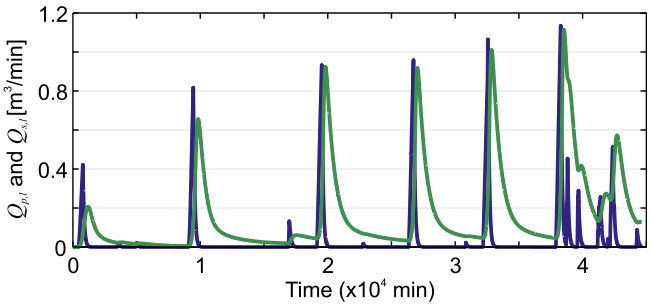

Fig. 6. Fluxes to the link calculated in m^3/min: the overland flux from ponded water $Q_{p,l}$ (solid blue) and the underground flux from the saturated soil $Q_{s,l}$ (solid green). (For interpretation of the references to color in this figure caption, the reader is referred to the web version of this article.)

very fast (Fig. 5(b) and (c)). We call the term $E(t)p(t)$ *evaporation from the ponded water* in a more general way, according to the following assumption: the vegetation on the hillslope absorbs a percentage E of the precipitation transferred to the ponded water reservoir, and the percentage depends on the pre-exiting conditions on the hillslope (for example, air humidity, temperature, plants' need for water) so it is variable in time, $E = E(t)$. Therefore, the term $E(t)p(t)$ contributes to the dynamics of s_p only during rain events, leaving $(1 - E(t))p(t)$ as the effective input (Fig. 5a: here $p(t)$ was recalculated in mm/min). The evapo-transpiration term $(E(t)p(t) + Q_{evap}/A_H)$ is then plotted in Fig. 5(d).

4.2.3. Dynamics of the runoff transport

The relative contribution of the overland flow and the underground flux to the runoff transport is illustrated in Fig. 6. These graphics correspond to the unit-adjustments to m^3/min of two important fluxes (see system (2) and Table 3): $Q_{p,l} = c_1 A_H s_p (a - a_{res} + v - v_{res})$ and $Q_{s,l} = c_2 A_H (a - a_{res}) \exp\left(\alpha_N \frac{a - a_{res}}{h_b}\right)$ (Fig. 6; curves in solid blue and solid green, respectively).

Between consecutive rain events, the dynamics of the runoff transport is governed by the underground flux from the saturated zone $Q_{s,l}$, to which Q tends asymptotically. Note that the main parameter that influences the slope of $Q_{s,l}$ is c_2, and in particular

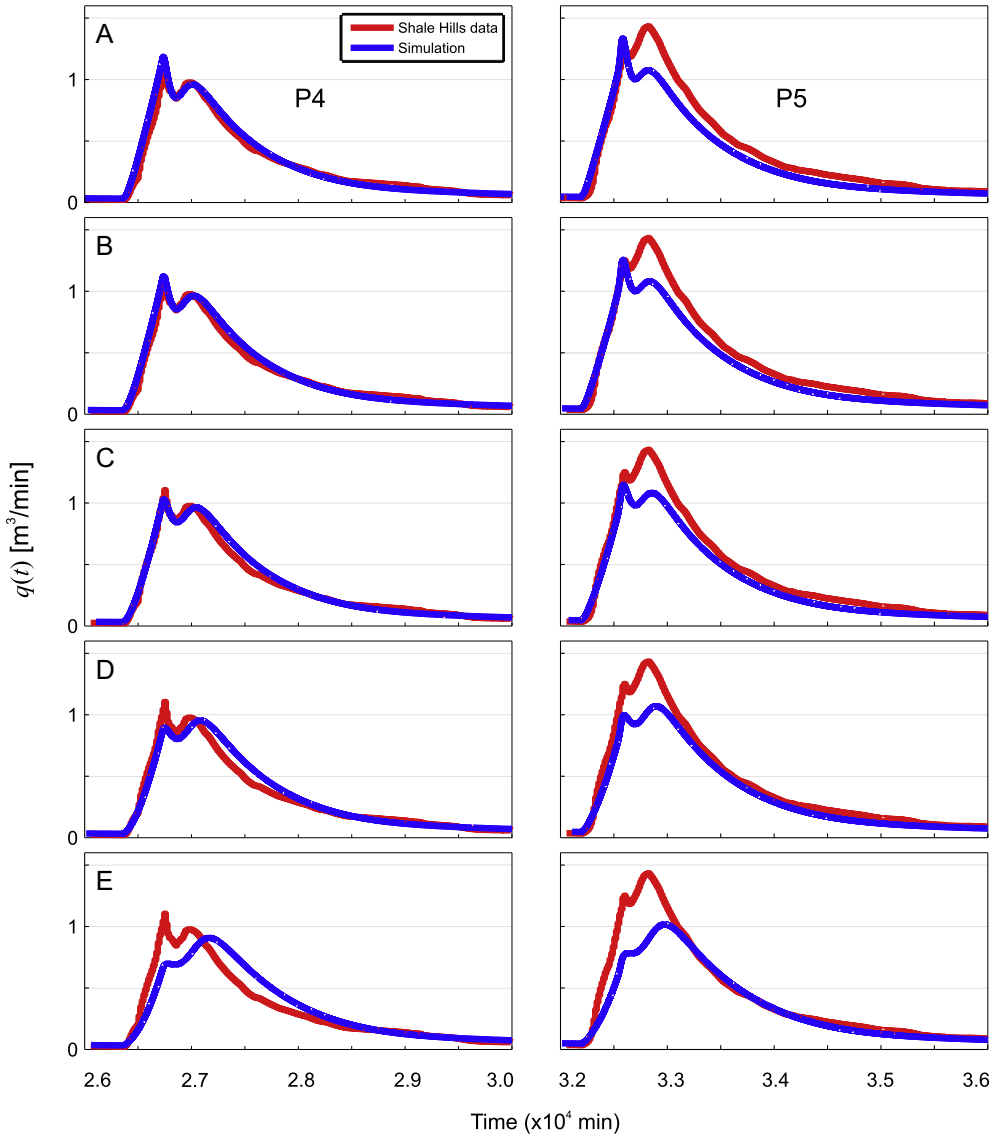

Fig. 7. Zoom in at peaks 4 and 5 of the simulated output flow $Q = qQ_r$ (solid blue) and comparison with Shale Hills data (solid red). Flow Q is determined using the parameter values and initial conditions from Section 4.1 except for K_{s_p}: (A) $K_{s_p} = 0.75$; (B) $K_{s_p} = 0.625$ (same as in Fig. 4); (C) $K_{s_p} = 0.50$; (D) $K_{s_p} = 0.375$; (E) $K_{s_p} = 0.25$. (For interpretation of the references to color in this figure caption, the reader is referred to the web version of this article.)

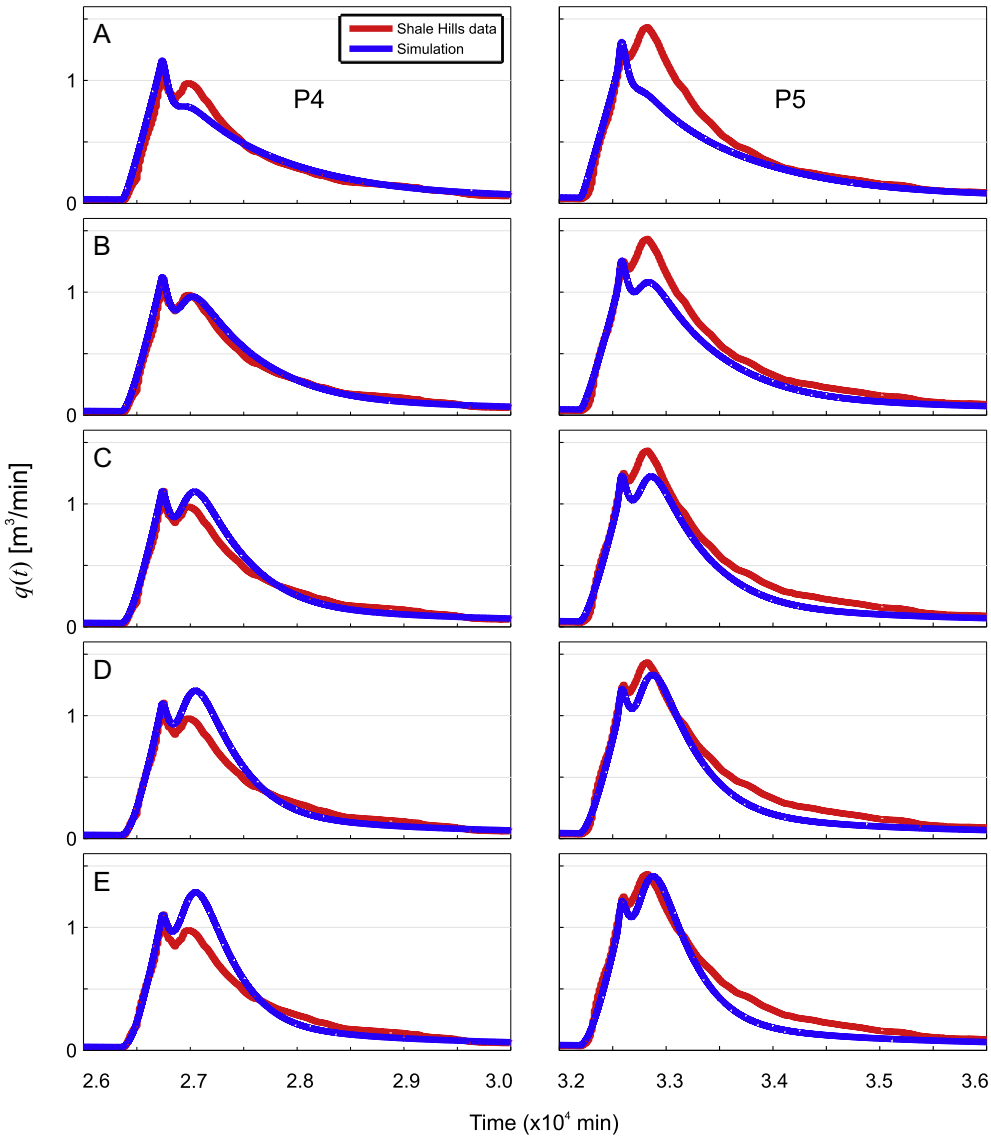

Fig. 8. Zoom in at peaks 4 and 5 of the simulated output flow $Q = qQ_r$ (solid blue) and comparison with Shale Hills data (solid red). Flow Q is determined using the parameter values and initial conditions from Section 4.1 except for α_{soil}: (A) $\alpha_{soil} = 3.125$; (B) $\alpha_{soil} = 5.0$ (same as in Fig. 4); (C) $\alpha_{soil} = 6.875$; (D) $\alpha_{soil} = 8.750$; (E) $\alpha_{soil} = 10.625$. (For interpretation of the references to color in this figure caption, the reader is referred to the web version of this article.)

α_{soil}. On the other hand, during each (6-h long) precipitation event, Q tends to the sum $(Q_{p,l} + Q_{s,l})$. The rise of Q is initially governed by $Q_{p,l}$ since s_p increases faster than a; at this stage, the main contribution of $Q_{s,l}$ is to set the maximum value that Q tries to reach rather than to significantly influence the slope of Q. A larger value of parameter c_2 (and so α_{soil}) would raise the peak of Q, while a smaller value of c_2 (α_{soil}) would lower it. (But note that changing c_2 would also affect the slope of Q in the time-interval between rain events. Therefore, c_2 needs to be carefully selected in order to obtain a reasonable fit for Q in both time-regimes; there is a trade-off for the best fitting of the runoff transport's *peak* versus its *decay*).

At the end of the rain event, s_p decreases rapidly and drives $Q_{p,l}$ to zero (see blue curve in Fig. 6) while $Q_{s,l}$ keeps increasing. Initially, the sum $(Q_{p,l} + Q_{s,l})$ (and Q asymptotically) follows the trend of $Q_{p,l}$ since this term is dominant ($Q_{p,l}$ is quadratic in variables s_p and a while $Q_{s,l}$ is basically linear in a for a in the neighborhood of a_{res}). That sets the initial decaying slope for Q. However, once the influence of $Q_{p,l}$ fades away ($Q_{p,l} \approx 0$), Q tends to $Q_{s,l}$, which is close to the end of its increasing phase. The combined effect is the occurence of a double peak in the dynamics of the runoff transport (see Figs. 6 and 4 for comparison with data).

Note that numerically, in order to obtain the double peak of Q, a balanced choice of values for coefficients c_1 and c_2 is necessary. Thus, for a given value of c_2 (α_{soil}), adjustments to c_1 can be made by an appropriate choice of the parameter K_{s_p}. Fig. 7 depicts snapshots of the fourth and fifth peaks in the simulation of the runoff transport when K_{s_p} varies. If K_{s_p} decreases while α_{soil} is kept fixed ($\alpha_{soil} = 5.0$), the first component of the double-peak of Q decreases. Note that reducing K_{s_p} past a certain value makes it disappear completely. (The second component of the double-peak seems less sensitive to K_{s_p}.) On the other hand, we can keep c_1 unchanged (i.e., $K_{s_p} = 0.625$) while modifying c_2 through the free parameter α_{soil}. Fig. 8 depicts snapshots of the fourth and fifth peaks in the simulation of the runoff transport when α_{soil} varies. Note that both components of the flow double-peak are affected by an increase in α_{soil} (they both rise), but this time the second component seems to be the most affected.

The variation of other parameters most probably influences the dynamics of the ODE system (3), too. However, we leave the careful

and detailed investigation of the parameter space of (3) and its associated dynamics for future research.

5. Discussion and conclusions

We developed a system of ordinary differential equations to reproduce simultaneously the aggregated behavior of changes in water storage in the hillslope surface and the unsaturated and saturated soil layers. The system of equations can be viewed as a two-state integral-balance model for soil moisture and groundwater dynamics [6]. We showed that fluxes between the unsaturated and saturated soil compartments can be described using a Taylor expansion of the underlying storage flux relationship. The model was tested using data collected in the Shale Hills watershed, a 7.9-ha forested site in central Pennsylvania, during an artificial drainage experiment in August 1974 where soil moisture in the unsaturated zone, groundwater dynamics and surface runoff were carefully monitored. Although more recent data is available for the Shale Hills experimental watershed (see [13]), we chose the 1974 data set because it removes all uncertainty associated with rainfall inputs from our data analysis and modeling exercise. The artificial drainage experiment provides the best opportunity to test the simplified assumptions used in our model.

The simplified ODE system given by (3) can reproduce data as closely as a PDE model (see [23]) when spatial averaging is considered along the hillslope. The state variables considered were streamflow at the outlet weir (flux q), the total volume of water in the soil, both in the unsaturated zone (v) and the saturated zone (a). We were particularly interested in being able to simulate the observed double peak in the hydrograph created after each rainfall event The appearance of the double peak in the ODE model is especially interesting because, at the very least, it provides an alternative to the hypothesis that the double peak should be the result of the hillslope's complex topography. Our results indicate that the appearance of the double peak in the spatially averaged ODE model is a consequence of the interaction between the hillslope overland runoff and the subsurface flow. Those seem to be in a delicate balance in order to produce the double peak.

The ODE model can also capture the qualitative and the quantitative dynamics of the underground water and offers a possible interpretation of how water is redistributed between the saturated and unsaturated zones between successive rainfall events. In the present configuration of the model structure, surface runoff is produced via infiltration excess overland flow, and the dynamical system offers an alternative hypothesis to the origin of the first peak in the hydrograph. Qu and Duffy [23] have argued, "During most of the numerical experiment, the soil infiltration capacity is large enough to accommodate rainfall, and Hortonian flow is of limited importance except in the upland regions during the fifth and sixth events. Saturation overland flow occurs at locations where water table saturates the land surface from below." See Fig. 12 in their paper. A careful inspection of the well data in the watershed does not support the conclusion, lending credibility to our model-based assessment of infiltration excess overland flow. It is necessary to qualify the extent to which our results apply. For example, the artificial rainfall applied and the time of the year in which the experiment was performed create a narrow range of hydro-climatic conditions in which this model is evaluated. Extreme drought or wet conditions in the soil can give rise to conditions that do not allow for ODE simplifications.

The approach we take in our paper leaves open the question of model parametrization (i.e., how are the parameters in the model related to physical soil properties?). However, the close match provided by PDE and ODE can become a tool with which to investigate this issue systematically. In addition, our ODE model can be easily coupled to a river network transport equation [9,20] to describe fluxes at the watershed scale, which would allow for a systematic investigation into how nonlinearities at the hillslope scale propagate producing fluctuations in the streamflow at the outlet of a watershed. This is the subject of future communications.

Why are these intermediate findings worth reporting? First, they represent a number of puzzles. Is it generally true that a good representation of surface and subsurface water dynamics cannot be achieved using a priori parameter values derived from available data without calibration? Or is this because our integration scale is not appropriate? Or, is it that there is something peculiar at this site that our models fail to capture? Second, while our goal is not to introduce a new hydrological model, we do want to provide an ODE-based framework that is flexible enough to simulate the underlying physical system while preserving the meanings of fluxes and state variables. We have achieved this, lending support for continuing the line of research that aims to simplify the description of a physical process at the hillslope scale of aggregation.

Appendix A. Water balance

The purpose of this section is to provide our analysis of data collected in Shale Hills during the 1974 artificial drainage experiment. We deemed this necessary because data itself offers some interesting hydrologic puzzles that needed to be sorted out before proceeding with the modeling exercise. Our primary modeling assumption is that the Shale Hills basin is a closed control volume and, thus, the equation

$$\frac{dS(t)}{dt} = p(t) - e(t) - q(t) \tag{A.1}$$

holds for any time t. Here, S is the total storage of water in the catchment, $p(t)$ is precipitation, $e(t)$ is evaporation and $q(t)$ is the discharge measured at the outlet (Weir 1). Integration of Eq. (A.1) gives,

$$\Delta S(t) = \int_0^{\Delta T} p(t)dt - \int_0^{\Delta T} e(t)dt - \int_0^{\Delta T} q(t)dt. \tag{A.2}$$

Eq. (A.2) can be directly tested using data collected during the artificial drainage experiment, which includes rainfall values, surface runoff measured at the basin outlet with a calibrated concrete weir and changes in the water content in the subsurface using an array of 44 wells and daily measurements of water content in the unsaturated zone using neutron probes. We estimated these variables by averaging the measurements available in the study area [13]. To estimate water volume in the saturated zone, we convert the water table depths (water table altitude measured by the piezometers minus the altitude of the bedrock) to volume of water in the saturated layer by assuming soil porosity equal to 0.4; see [13]. The volume of water in the unsaturated zone was estimated based on the 40 neutron probes. Evett and Steiner [8] provide details about the neutron probe method to measure soil moisture in the unsaturated zone. After calibration, these instruments provide the average water content over a vertical soil profile. Fig. A.9(a) shows graphs of cumulative values of precipitation and runoff as a function of the accumulation period. Fig. A.9(b) shows values of $\Delta S = S(t) - S(0)$. The unmeasured component in the water balance during the experiment is evaporation. Note that Eq. (A.2) can be rearranged to estimate the total water loss (evaporation from subsurface and water losses in the surface). In addition, we recognize that heterogeneities in the soil matrix porosity and areas inaccessible to water (e.g., portions of soil matrix occupied by tree roots, gravel, etc.) can change the magnitude of subsurface water level fluctuations. We also recognize that

evaporation from the surface can be a significant portion of the water entering the soil matrix. In the artificial drainage experiments, water is applied on sunny days, making water captured by temporary interception zones more likely to evaporate than during actual precipitation events. We introduce two variables, β and $\alpha(t)$ to account for those two issues and rewrite Eq. (A.2) as,

$$\int_0^{\Delta T} e(t)dt = \int_0^{\Delta T} \alpha(t)p(t)dt - \int_0^{\Delta T} q(t)dt - \beta\Delta S(t). \tag{A.3}$$

Conversely, if daily evaporation is assumed to be known (e.g., 4 mm/day), $\alpha(t)$ can be derived from data as (i.e., assuming $\alpha(t)$ is constant over the day),

$$\alpha(t) = \frac{\beta\Delta S(t) + \int_t^{t+\Delta T'} e(t)dt + \int_t^{t+\Delta T'} q(t)dt}{\int_t^{t+\Delta T'} p(t)dt}. \tag{A.4}$$

The need to introduce β and $\alpha(t)$ will become evident as we present the data analysis.

First, we calculate cumulative evaporation using Eq. (A.3) assuming $\alpha(t) = 1$ and choosing an arbitrary initial $S(0) = 0.35$. Note in Fig. A.9(c) that when β is assumed to be 1, the water balance gives a non-increasing evaporation function. In fact, when daily evaporation rates are estimated, it yields either negative values of evaporation or non-realistic positive evaporation values during days of large precipitation events. This situation can be significantly improved if a value of β smaller than 1 is assumed. In fact, when we assume β on the order of 0.1, we get an average evaporation rate on the order of 4 mm/day, which is consistent with evaporation values for the region (4.6 mm/day; see [10]). In a second step, we relax the assumption that $\alpha(t) = 1$ and calculate the value needed to close the water balance, assuming that evaporation is constant and equal to 4.6 mm/day. The values of $\alpha(t)$ are shown in Fig. A.9(d). Our analysis leads us to believe that two physical phenomena combine to explain the variability in data: first, that there is a significant portion of the soil matrix that is not accessible to water, leading to large changes in the water table depth when small rainfall amounts are applied in the system, and second, that water losses from the surface, either by direct runoff or evaporation, occur during the application of the artificial rainfall (here, we take the measured values to be error-free since going back to the original references gives us confidence that the measurements are accurate within the range provided by the instruments).

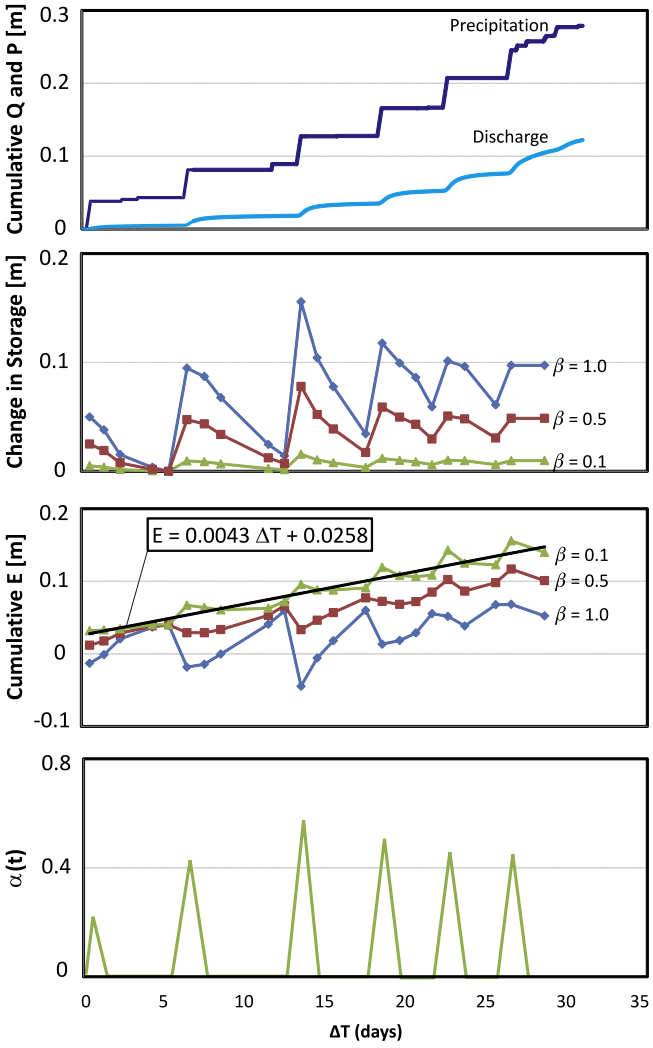

Fig. A.9. (a) Cumulative precipitation and runoff derived from measurements in the Shale Hills basin, (b) Estimated soil water contents, (c) Estimated evaporation from the system required to close the water balance with different values of β and (d) Estimated fraction of water loss $\alpha(t)$ assuming a constant evaporation rate of 4.6 mm/day.

Appendix B. Fluxes and parameters of a more parsimonious integral-balance ODE system

The fluxes from system (1) are defined by

$$q_{pl} = c_2\frac{a_P RC + a_I}{A_H}v_h s_p, \quad q_{pu} = \frac{a_P}{A_H}(1 - RC)\ In\ f\ Rate,$$
$$q_{us} = 10^3 K_{UNSAT}\theta\left(\frac{a_P}{A_H}\right), \quad q_{sl} = c_3 v_{s_{sat}}\left(\frac{a_I}{A_H}\right)$$

with parameters, constants and other related formulas listed in Tables B.6 and B.7.

Parameter values for $L_h, A_H, A_{up}, S_H, H_h, a, b, c$ were obtained from DEM, and h_b is equal to the average soil water capacity divided by the hillslope area. Taking into consideration our discussion in A, h_b is equal to the average soil depth times the soil porosity and the variable β; *MaxInf* and K_{SAT} were obtained based on soil datasets (SSURGO), and n is the Manning roughness coefficient for forested

Table B.6
Shale Hills parameters in model (1) from [4].

Parameter	Value	Unit	Physical interpretation
$A_{upstream}$	0.07736019	km^2	Upstream area
A_H	0.07736019	km^2	Hillslope area
L_h	0.4201452	km	Channel length
h_b	69	mm	Effective depth to the impermeable layer
λ_1	0.25		Discharge exponent for flow velocity
λ_2	−0.1		Area exponent for flow velocity
v_0	0.02	m/s	reference velocity
K_{SAT}	0.01	m/h	Saturated hydraulic conductivity
K_T	1.0	m/h	Conductivity for infiltration
C_r	0.4		Channel geometry coefficient
e_{pot}	0.2	mm/h	Potential evaporation
H_h	49.01019	m	Hillslope relief
MaxInf	76.2	m/h	Maximum infiltration rate
S_H	0.11		Hillslope slope
n_{vh}	0.4		Manning coefficient
a	0.0		Parameters a, b, c and d are coefficients
b	0.487372		of the third order polynomial that
c	2.458623		describes the relationship between the
d	−1.94599		impermeable area and the water table (based on the convexity shape of the hillslope)

Table B.7
Formulas and other important constants in model (1) from [4].

Formula	Unit	Physical interpretation
$d_{soil}(\theta) = (1-\theta)h_b$	mm	Soil deficit
$K_{UNSAT}(\theta) = K_{SAT}e^{b_{soil}(\theta-1)}$	m/h	Unsaturated hydraulic conductivity
$v_h = c_1(s_p \cdot 10^{-3})^{2/3}$	m/h	Hillslope velocity
$RC(s_p, d_{soil}) = \left(\frac{s_p(s_p+2d_{soil})}{(s_p+d_{soil})^2}\right)$	no unit	Runoff coefficient
$Inf\ Rate = \begin{cases} MaxInf \\ \text{if } s_p > MaxInf \\ K_T s_p \ otherwise \end{cases}$	mm/h	Infiltration
$h_{rel}(h_w) = h_w - h_b$	m	Relative water depth
$a_I(h_{rel}) = A_H\left[a + b\left(\frac{h_{rel}}{H_{relmax}}\right) + c\left(\frac{h_{rel}}{H_{relmax}}\right)^2 + d\left(\frac{h_{rel}}{H_{relmax}}\right)^3\right]$	km^2	The impermeable area
$\frac{da_I}{dh_{rel}}(h_{rel}) = \frac{A_H}{H_{relmax}}\left[b + 2c\left(\frac{h_{rel}}{H_{relmax}}\right) + 3d\left(\frac{h_{rel}}{H_{relmax}}\right)^2\right]$	km^2/m	The change in impermeable area
$a_P(a_I) = A_H - a_I$	km^2	The permeable area
$v_{s_{sat}}(a_I) = h_b a_I$	m^3	Volume of soil that is saturated
$v_{s_{unsat}}(v_{s_{sat}}) = V_T - v_{s_{sat}}$	m^3	Volume of soil that is unsaturated
$v_{w_{unsat}}(\theta, v_{s_{unsat}}) = \theta v_{s_{unsat}}$	m^3	Volume of water in the unsaturated layer of soil
$\overline{D}_{unsat} = 10^{-3}\left(\frac{v_{s_{unsat}}}{A_H}\right)$	mm	The average water depth in the unsaturated layer
$\overline{D}_{sat} = 10^{-3}\left(\frac{v_{s_{sat}}}{A_H}\right)$	mm	The average water depth in the saturated layer
Constant	**Unit**	
$A_r = 1$	km^2	
$Q_r = 1$	m^3/s	
$H_{relmax} = H_h$	m	
$K_q = \frac{60C_r v_0 (A_{up}/A_r)^{\gamma 2}}{(1.0-\lambda_1)L_h}$	min^{-1}	
$V_T = 10^3\ h_b\ A_H$	m^3	
$c_1 = \frac{3.6\cdot 10^6}{n_{reh}}\sqrt{S_H}$	m/h	
$c_2 = (2\cdot 10^{-6})\frac{L_H}{A_H}$	m^{-1}	
$c_3 = \frac{10^3}{V_T}K_{SAT}S_H$	mm/(h m^3)	
$c_4 = \frac{1}{3.6}A_H$	(m^3 h)/(s mm)	
$c_5 = \frac{10^6}{60}\frac{A_H}{h_b}$	(m h)/ min	
$c_6 = \frac{10^3}{60}A_H$	m^3 h/(min mm)	
$c_7 = \frac{1}{60}$	h/min	
$c_8 = \frac{10^3}{60}$	(m h)/(mm min)	

area. We estimate λ_1 and λ_2 based on velocity measurements data provided by the USGS – see [4] for details. As this dataset does not comprise data for hillslopes (just for watershed larger than 10 km^2), we estimate v_0 based on the average hillslope concentration time (time difference between the peak of rainfall and the peak of streamflow) and flow path. We recognize that this is not the most appropriate methodology to estimate v_0, since it requires rainfall and streamflow measurement; therefore, it cannot be applied to ungauged basins. In other studies, for which velocity measurement data are available at the appropriate scales [5], we estimate all velocity parameters solely based on such measurements.

Evaporation is defined based on potential evaporation and the amount of water available in the different hillslope storages: surface and soil in the portion of the basin where it is impermeable (water is easily available) and permeable (evaporation will be a function of soil volumetric water content). We first estimate C_p, C_{unsat}, C_{sat}, which represent the water that would evaporate from these storages if potential evaporation were infinite. Thus, if $e_{pot}(t) > 0$ then $C_p = \frac{s_p}{(1\ hr)e_{pot}}$, $C_{unsat} = \frac{\overline{D}_{unsat}\theta}{h_b}\frac{a_P}{A_H}$, $C_{sat} = \frac{\overline{D}_{sat}}{h_b}\frac{a_I}{A_H}$. Otherwise: $C_p = C_{unsat} = C_{sat} = 0$. We then correct the values based on the actual potential evaporation: say $C_T = C_p + C_{unsat} + C_{sat}$; if $C_T > 1$ then $Corr = (C_p + C_{unsat} + C_{sat})^{-1}$ and otherwise $Corr = 1$. Now we define e_p, e_{sat}, e_{unsat}, the evaporation rates from the surface, saturated layer and unsaturated layer, in $[mm/h]$ by: $e_p = Corr\, C_p\, e_{pot}$, $e_{sat} = Corr\, C_{sat}\, e_{pot}$, $e_{unsat} = Corr\, C_{unsat}\, e_{pot}$.

Appendix C. Definition of fluxes in the nonlinear hillslope-link model

Definition of fluxes $Q_{p,l}$ and $Q_{p,u}$. Given a precipitation input $p(t)$, the change in the land surface storage volume depends on the incoming flux $A_H p(t)$ minus a total water loss $E(t)$ due to rapid evaporation from the surface or interception by vegetation, and it is expressed as a percentage from the incoming water (i.e. $-E(t)A_H p(t)$) and the fluxes $Q_{p,l}$ and $Q_{p,u}$ that move the ponded water to the channel link (surface runoff) and into the unsaturated

zone (infiltration), respectively. That means $d(A_H s_p)/dt = A_H ds_p/dt = (1-E(t))A_H p(t) - Q_{p,l} - Q_{p,u}$ or, equivalently, $ds_p/dt = (1-E(t))c_3 p(t) - \frac{1}{A_H}(Q_{p,l}+Q_{p,u})$. The input function $p(t)$ is given in (mm/h), so a dimensionless coefficient c_3 is introduced to adjust the units and is defined by $c_3 = 10^{-3}/60$. Typically, the land surface storage s_p is measured in millimeters ranging from 0 to 1000 mm, but here we will use meters as the unit for s_p. Thus, a typical interval for s_p is expected to be [0 m,1 m]. The fluxes $Q_{p,l}$ and $Q_{p,u}$ need to be a function of the variables in the system to provide closure relationships. In order to do this, we make the assumption that, in the absence of rainfall, the above equation can be modeled as,

$$\frac{ds_p}{dt} = -K_{s_p} s_p^{\gamma}. \tag{C.1}$$

The assumption of a power law decay is in agreement with direct observations [26]. Note that Eq. (C.1) can be obtained from a simple recalculation of an equation of the form $ds_p/dt = -\widehat{K}_{s_p}\left(\frac{A_H s_p}{V_{tot}}\right)^{\gamma}$ with coefficient $\widehat{K}_{s_p}$ measured in $\mathrm{m}\times\mathrm{h}^{-1}$ and total volume V_{tot} measured in $\mathrm{m}\times\mathrm{km}^2$. Therefore, $K_{s_p} = \widehat{K}_{s_p}(A_H/V_{tot})^{\gamma} = \widehat{K}_{s_p} h_b^{-\gamma}$ would be a recession coefficient measured in $\mathrm{m}^{1-\gamma}\times\mathrm{h}^{-1}$.

We also assume that the flux $Q_{p,u}$ is proportional to both the volume stored on the land surface $v_{w-ponded} = A_H s_p$ and the available soil deficit volume $v_{soil}^{def} = V_T - v_{w-sat} - v_{w-unsat} = \beta A_H(h_b - a - v)$ So $Q_{p,u}$ is given by the equation: $Q_{p,u} = A_H \widehat{K}_{s_p}\left(\frac{A_H s_p}{V_{tot}}\right)^{\gamma}\frac{\beta A_H(h_b-a-v)}{V_T} = \frac{K_{s_p}\beta A_H^2}{V_T} s_p^{\gamma}(h_b-a-v)$. Thus, the formula for $Q_{p,u}$ becomes $Q_{p,u} = \frac{K_{s_p}A_H}{h_b} s_p^{\gamma}(h_b-a-v)$.

In order to satisfy Eq. (C.1), the sum of fluxes coming out of the ponded water during periods of no rain needs to satisfy $\frac{1}{A_H}(Q_{p,u}+Q_{p,l}) = K_{s_p} s_p^{\gamma}$ thus $\frac{K_{s_p}A_H}{h_b} s_p^{\gamma}(h_b-a-v) + Q_{p,l} = A_H K_{s_p} s_p^{\gamma}$ and we define $Q_{p,l} = K_{s_p} A_H s_p^{\gamma}\frac{\beta A_H(a+v)}{V_T} = \frac{K_{s_p}\beta A_H^2}{V_T} s_p^{\gamma}(a+v) = \frac{K_{s_p}A_H}{h_b} s_p^{\gamma}(a+v)$. We take $\gamma = 1$ as a first approximation, and we subsequently show that it is sufficient to simulate overland flow and infiltration. At this point, we need to take into account the following important observation about the dynamics of the hydrological system, given the time-interval of the study (one month or maybe several months). The above definitions of $Q_{p,u}$ and $Q_{p,l}$ are phenomenological, so they should apply during very long periods of time (for example, centuries). An extended lack of precipitation for such a long time-interval ($p(t) = 0$) brings the ODE system to a steady state, with variables a and v tending to zero. However, this is not really the case with the hydrological system under study, since even in the complete absence of precipitation ($p(t) = 0$), there is still residual water in the soil. Therefore, a more reasonable assumption is to consider non-zero steady states for the variables a and v, say a_{res} and v_{res}. A shift of variables a and v to their steady-state values in $Q_{p,u}$ and $Q_{p,l}$, according to $a \mapsto a - a_{res}$ and $v \mapsto v - v_{res}$, is imposed. This allows us to re-write $Q_{p,u}$ and $Q_{p,l}$, as in Table 3, to account for the residual water in the soil.

Definition of flux $Q_{s,l}$ It is defined by the product between the cross-sectional area $A_{SL} = 2\times Lh_b$ (where L is the length of the channel and h_b is the effective soil depth) and the velocity $vel_s = K_{SAT}\mathcal{F}$. The constant K_{SAT} is the saturated hydraulic conductivity (measured in [m/h]). The function $\mathcal{F}$ (dimensionless) depends on the volume of water in the saturated soil ($v_{w-sat}/V_T = \beta a A_H/(\beta h_b A_H) = a/h_b$), and it should satisfy $\mathcal{F} = 0$ at the equilibrium $a = a_{res}$. Thus, we define $\mathcal{F} = \mathcal{F}(x)$ with $x = (a - a_{res})/h_b$. In order to account for the original, more complicated geometry of the cross-sectional area between the saturated soil and the channel, we introduce a correction factor α_{soil} (dimensionless) and have $Q_{s,l} = A_{SL}\, vel_s = \alpha_{soil} 2Lh_b K_{SAT}\mathcal{F}(x)$. A qualitative analysis of the hydrograph recessions indicate that a linear form $\mathcal{F}(x) = x$ is not sufficient to reproduce the complex dynamics of the flux $Q_{s,l}$. This is because the hillslope saturated zone has a more intricate geometry than the rectangular parallelepiped of base-area A_H and height h_b that we consider here. Thus, including higher order nonlinearities in the definition of $\mathcal{F}$ seems important, and we therefore choose a function $\mathcal{F}$ that decreases *linearly* with x in the neighborhood of the origin ($\mathcal{F} = \mathcal{O}(x)$ as $x \to 0$) but that otherwise increases *exponentially fast* with x : $\mathcal{F}(x) = xe^{\alpha_N x}$. Therefore, the flux $Q_{s,l}$ is defined by $Q_{s,l} = \alpha_{soil} 2Lh_b K_{SAT}\frac{a-a_{res}}{h_b}\exp\left(\alpha_N\frac{a-a_{res}}{h_b}\right) = c_2 A_H(a-a_{res})\ \exp\left(\alpha_N\frac{a-a_{res}}{h_b}\right)$ with coefficient c_2 accounting for the units, too.

There is a direct connection between the exponential function and high degree polynomial given by a Taylor expansion, by recalling that the Taylor expansion of $e^{\alpha_N x}$ about the origin is $e^{\alpha_N x} = \sum_{n=0}^{\infty}\frac{\alpha_N^n}{n!}x^n$. So, obviously, the function $\mathcal{F}(x)$ can be interpreted as an infinite polynomial containing all possible high order nonlinearities. We do not claim that the same accuracy for fitting cannot be achieved by a high degree polynomial; however, we prefer to work with the exponential function since it has much more convenient mathematical properties.

Definition of flux Q_{evap} We also account for potential loss of groundwater through evapotranspiration by introducing a flux Q_{evap} proportional to the volume of water in the saturated zone, $Q_{evap} = K_{evap} A_H(a - a_{res})$. Here, K_{evap} is a very small recession coefficient measured in (h^{-1}) so $Q_{evap} = c_{evap} A_H(a - a_{res})$ with coefficient c_{evap} defined by (4).

References

[1] Apip, Sayama T, Tachikawa Y, Takara K, Yamashiki Y. Assessing sources of parametric uncertainty and uncertainty propagation in sediment runoff simulations of flooding. J Flood Risk Manage 2010;3:270–84.

[2] Brandes D, Duffy C. Stability and damping in a dynamical model of hillslope hydrology. Water Resour Res 1998;34(12):3303–13.

[3] Carpenter T, Georgakakos K. Intercomparison of lumped versus distributed hydrologic model ensemble simulations on operational forecast scales. J Hydrol 2006;329:174–85.

[4] Cunha LK. Exploring the benefits of satellite remote sensing for flood prediction across scales [Ph.D. thesis]. The University of Iowa, Department of Civil and Environmental Engineering; 2012.

[5] Cunha LK, Mandapaka PV, Krajewski WF, Mantilla R, Bradley AA. Impact of radar-rainfall error structure on estimated flood magnitude across scales: an investigation based on a parsimonious distributed hydrological model. Water Resour Res 2012;48:W10515. http://dx.doi.org/10.1029/2012WR012138.

[6] Duffy C. A two-state integral-balance model for soil moisture and groundwater dynamics in complex terrain. Water Resour Res 1996;32:2421–34.

[7] Ermentrout B. Simulating, analyzing, and animating dynamical systems: a guide to XPPAUT for researchers and students. Software environment and tools, vol. 14. Philadelphia: SIAM; 2002.

[8] Evett SR, Steiner JL. Precision of neutron scattering and capacitance type soil water content gauges from field calibration. Soil Sci Soc Am J 1995;59:961–8.

[9] Formetta G, Mantilla R, Franceschi S, Antonello A, Rigon R. The jgrass-newage system for forecasting and managing the hydrological budgets at the basin scale: models of flow generation and propagation/routing. Geosci Model Dev 2011;4(4):943–55.

[10] Fulton JW, Koerkle EH, McAuley SD, Hoffman SA, Zarr LF. Hydrogeologic setting and conceptual hydrologic model of the spring creek basin, Centre County, Pennsylvania, June 2005. US geological survey scientific investigations report; 2005.

[11] Gupta VK. Emergence of statistical scaling in floods on channel networks from complex runoff dynamics. Chaos Soliton Fract 2004;19(2):357–65.

[12] Gupta VK, Waymire EC. Spatial variability and scale invariance in hydrologic regionalization. In: Sposito G, editor. Scale dependence and scale invariance in hydrology. Cambridge, UK: Cambridge University Press; 1998. p. 88–135.

[13] <http://www.pihm.psu.edu/applications.html>; 2012

[14] Kampf S, Burges S. Parameter estimation for a physics-based distributed hydrologic model using measured outflow fluxes and internal moisture states. Water Resour Res 2007;43:W12414. http://dx.doi.org/10.1029/2006WR005605.

[15] Kumar M. Toward a hydrologic modeling system [Ph.D. thesis]. The Pennsylvania State University, Department of Civil and Environmental Engineering; 2009.

[16] Lynch JA. Effects of antecedent moisture on storage hydrographs [Ph.D. thesis]. Pennsylvania State University, Department of Forestry; 1976.

[17] Lynch JA, Corbett W. Source-area variability during peakflow, in watershed management in the 80s. J Irrig Drain Eng 1985:300–7.
[18] Mandapaka PV, Villarini G, Seo B, Krajewski W. Effect of radar-rainfall uncertainties on the spatial characterization of rainfall events. J Geophys Res: Atmos 2010;115:D17110. http://dx.doi.org/10.1029/2009JD013366.
[19] Mantilla R. Physical basis of statistical scaling in peak flows and stream flow hydrographs for topologic and spatially embedded random self-similar channel networks [Ph.D. thesis]. University of Colorado, Boulder, Department of Civil and Environmental Engineering; 2007.
[20] Mantilla R, Gupta VK, Mesa O. Role of coupled flow dynamics and real network structures on Hortonian scaling of peak flows. J Hydrol 2006;322(1–4):155–67.
[21] Mascaro G, Vivoni ER, Deidda R. Implications of ensemble quantitative precipitation forecast errors on distributed streamflow forecasting. J Hydrometeorol 2010;11:69–86.
[22] Menabde M, Sivapalan M. Linking space-time variability of rainfall and runoff fields on a river network: a dynamic approach. Adv Water Resour 2001;24:1001–14.
[23] Qu Y, Duffy C. A semidiscrete finite volume formulation for multiprocess watershed simulation. Water Resour Res 2007;43(W08419):1–18.
[24] Reggiani P, Sivapalan M, Hassannizadeh SM, Gray W. Coupled equations for mass and momentum balance in a stream network: theoretical derivation and computational experiments. Proc. R. Soc. London A 2001;457:157–89.
[25] Small SJ, Jay LO, Mantilla R, Curtu R, Cunha LK, Fonley M, Krajewski WF. An asynchronous solver for systems of odes linked by a directed tree structure. Adv Water Resour 2013;53:23–32.
[26] Teuling AJ, Lehner I, Kirchner JW, Seneviratne SI. Catchments as simple dynamical systems: experience from a swiss pre-alpine catchment. Water Resour Res 2010;46:W10502. http://dx.doi.org/10.1029/2009WR008777.